Nanoparticles in polymer-matrix composites

Sabine Schlabach · Rolf Ochs · Thomas Hanemann · Dorothée Vinga Szabó

Abstract Regarding the development of nanoparticles for polymer matrix composites the particle/agglomerate size and particle/agglomerate distribution in the composites, respectively, is often crucial. This is exemplarily shown for, e.g. optical applications with measurements of refractive index and transmittance. Classical blending techniques, where nanoparticles are dispersed in polymers or resins, are compared to a combination of a special gas-phase synthesis method with subsequent in-situ deposition of nanoparticles in high-boiling liquids. The particles/agglomerates were characterized regarding particle size and particle size distribution using transmission electron microscopy and dynamic light scattering. Additionally, important material properties like mechanical properties, relevant for application, or like viscosity, relevant for processing, are determined. It is shown, that with in-situ dispersed nanoparticles synthesized in a microwave plasma process composites with finely dispersed particles/agglomerates are attainable.

1 Introduction

Composites made from a polymer matrix containing functional nanoparticles as fillers gained increasing scientific and technological interest. In the last years several reviews have been published regarding this subject (Caseri 2006; Althues et al. 2007; Paul and Robeson 2008; Hanemann and Szabó 2010). With such composite materials a broad variety of applications can be covered, comprising optical, dielectric, electronic, magnetic, and mechanical properties of the polymer composite. Additionally, using nanoparticles as fillers opens new prospects, since many physical properties are size dependent (Han et al. 1994; Kyprianidou-Leodidou et al. 1994; Li et al. 2004; Qi and Wang 2005; Nienhaus et al. 2006; Luca 2009; Zhang et al. 2009; Doak et al. 2010). For a specific tailoring of composite properties, knowledge of functional properties of the filler material is mandatory. A good review concerning gas phase synthesized nanoparticles for electronic, optical and magnetic applications is given by Kruis et al. (1998).

Micro-optical devices with tailored refractivity are a challenging application of nano-modified composites. Therefore, polymer materials with active inorganic fillers, adjusting the polymer's optical properties, are of great technological interest, e.g. in the area of polymer waveguide devices, especially in the range of telecommunication ($\lambda = 1{,}300$ and $1{,}550$ nm). One way to adjust the optical properties of the composites is to embed inorganic nanoparticles with inherent high refractive index in a polymer. In this case, the particle size, respectively, agglomerate size, must be smaller than 1/10th of the applied wavelength to avoid Rayleigh scattering, because otherwise the transmittance is degrading. Many research groups work on this area, fabricating mainly TiO_2/polymer nanocomposites with modified refractive index (Nussbaumer et al. 2003; Guan et al. 2006; Nakayama and Hayashi 2007). Usually, chemical in-situ methods are used, generating the nanoparticles directly in a sol, with a subsequent

S. Schlabach (✉) · R. Ochs · T. Hanemann · D. V. Szabó
Institute for Materials Research III, Karlsruhe Institute of Technology, Hermann von Helmholtz Platz 1, 76344 Eggenstein Leopoldshafen, Germany
e mail: sabine.schlabach@kit.edu
URL: www.imf3.kit.edu

T. Hanemann
Department of Microsystems Engineering (IMTEK), University of Freiburg, Georges Koehler Allee 102, 79110 Freiburg, Germany

polymerization of the sol. These authors reach relatively high particle loading and high increase in refractive index, transmission of their samples usually is indicated only for thin films. Bulk nanocomposites synthesized by these methods are not described.

The second approach of composite formation is ex-situ fabrication of the composites, using externally synthesized nanoparticles which are blended to a polymer. Blending techniques are, e.g. stirring methods (Böhm et al. 2004) or, in case of thermoplastic melts, extruders have been often used for compounding (Hanemann et al. 2009). These methods lead to bulk composites. Unfortunately, commercial nanoparticles are often characterized by a broad particle size distribution and are typically agglomerated to sizes of several 100 nm. A sufficient deagglomeration is mostly impossible. To obtain an impression regarding particle size and particle size distribution of commercially available nanopowders, Fig. 1 shows exemplarily transmission electron microscopy (TEM) images of two different commercial nanopowders, and a nanocomposite made with commercial AEROSIL® R8200 nanoparticles, respectively. Using such particles the transparency of the composites is rapidly decreasing with increasing particle content due to Rayleigh scattering at either large particles, or large agglomerates.

Further interesting application potential for high quality nanoparticles is seen as microwave-active additives for a newly developed microwave-curing system for carbon fiber reinforced plastics (Feher 2009; Schlabach et al. 2009), as well as for ink-jet printing. In both application areas there is a need for small agglomerates (meaning for agglomerates with sizes significantly below 100 nm) and an inherent low tendency of agglomeration.

In this paper we will demonstrate the benefit of core/shell nanoparticles for application in optical microsystems, and the benefit of combining a non-thermal microwave plasma process with in-situ deposition of nanoparticles in liquids regarding agglomerate size. With the microwave plasma process nanoparticles with sizes typically <10 nm and narrow particle size distribution are attainable (Vollath and Szabó 2006). Another advantage of this process is the possibility of in-situ surface modification leading to hybrid core/shell particles (Vollath et al. 1999; Szabó et al. 2008). Benefits of surface modification are the combination of material properties in one particle as well as adaption to the matrix.

For the composite formulation two different routes are used. In the first approach several core/shell nanoparticles with PMMA-shell are blended into PMMA by standard mixing techniques. The organic shell is supposed to reduce agglomeration tendency of the ceramic cores after synthesis and modifies the particle-polymer interface. Hence, the coating is expected to facilitate the incorporation into the polymer resin yielding to particles/agglomerates not exceeding the critical size. In a second approach several bare as well as PMMA-coated nanoparticles are precipitated directly into a liquid. The main attention in characterization is paid on particle size and particle size distribution.

2 Experimental

2.1 Synthesis of nanoparticles

The Karlsruhe Microwave Plasma Process (KMPP), a non-thermal, low-pressure process, is very well suited for the synthesis of nanoparticles with particle sizes <10 nm and very narrow particle size distribution (Vollath and Szabó 2006). As a further advantage, it is possible to synthesize core/shell and multi-layer nanoparticles in manifold combinations. A detailed description of the process is given

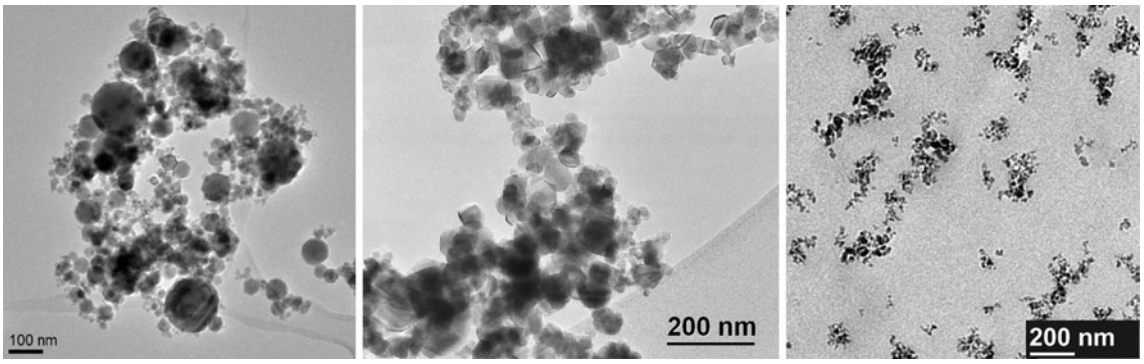

Fig. 1 TEM images of different, commercially available nanopow ders. *Left image* shows Fe_2O_3 nanoparticles, *middle image* shows SnO_2 nanoparticles (both Sigma Aldrich GmbH). In both cases the primary size of the particles ranges from about 5 nm to more than 100 nm. The agglomerates are several 100 nm in size. *Right image* shows a section of a nanocomposite made of PMMA and commercial AEROSIL® R8200 (Evonik Degussa GmbH) (Hanemann and Szabó 2010), characterized by agglomerates of several 100 nm in dimension

elsewhere (Vollath and Szabó 1999; Lamparth et al. 2002; Vollath and Szabó 2006).

In the standard set-up powders have been collected via thermophoresis. With a modified set-up direct precipitation of nanoparticles into liquids is possible. In this setup the process gas is directed through a flask filled with a liquid. Using the direct deposition into liquids, suspensions with strongly reduced tendency of particle agglomeration can immediately be obtained. Due to the working pressure, direct deposition is possible into high boiling liquids, polymers and resins. Figure 2 schematically shows the experimental setup for the synthesis of ceramic nanoparticles with the two applied particle collection methods.

The gas flow of the reaction gas (20% O_2 in Ar) was typically set to 5 l/min resulting in a system pressure of about 10 mbar. The thermal gradient for thermophoretic powder collection was realised using an outer heating jacket set to 300°C and an inner cooling finger operating with flowing tap water. The use of liquid nitrogen to increase thermal gradient is unsuitable, since reaction residuals in the offgas are collected, too. In case of in-situ deposition into liquids the liquids are equilibrated depending to their viscosity. Typically values used in this study are 80°C for the high viscosity liquids realised using a heating jacket and 10 20°C for the low viscosity liquids using a cooler system. The difference between the temperature of the gas stream directly measured behind the reaction zone and the temperature of the liquids was typically in the range of about 500°C. The efficiency of the thermophoretic powder collection method is typically in the range of 30 50% assuming entire precursor conversion. In case of direct precipitation into liquids the efficiency is around 10 15%. Both efficiencies are attainable without any optimization of the temperature gradient or the gas stream.

2.2 Composite formation

To prepare nanocomposites, either powder collected by thermophoresis (ex-situ) or particles directly deposited into liquids (in-situ) was used. Table 1 summarizes the relevant experimental data of particle synthesis and details of composite formation for the samples presented in this paper. In Table 2 some relevant physical data of the used components are given.

Ex-situ composite formation processes are, generally spoken, methods, where nanoparticles, synthesized in an external synthesis step, are added or mixed to a monomer or resin (organic solution), usually followed by a polymerization. In the simplest case the nanoparticles are used as produced or delivered, posing the most problems concerning agglomeration. For the ex-situ formation of composites in this study the mixing was done with a dissolver stirrer using a method described elsewhere (Ritzhaupt-Kleissl et al. 2005).

With the in-situ composite formation method the nanoparticles are directly deposited into a liquid. When this liquid is a resin and contains the desired nanoparticles it is directly curable after addition of hardener. Another possibility is the in-situ-deposition into reactive diluents which are processible after addition of appropriate amounts of resin and hardener.

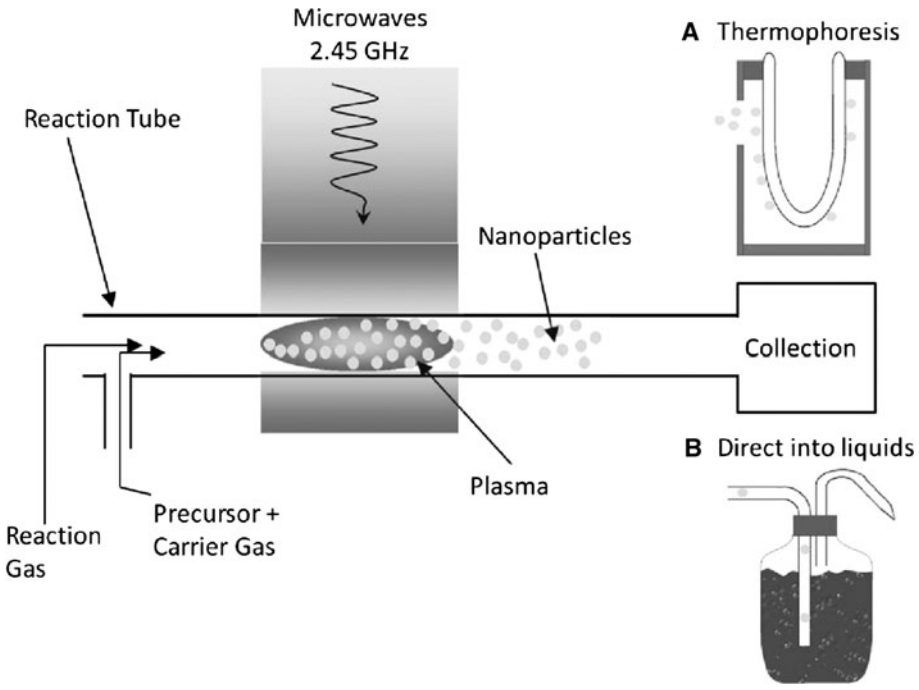

Fig. 2 Principle of the microwave plasma synthesis of nanoparticles with the two powder collection methods thermophoresis (*A*) and directly into liquids (*B*)

Table 1 Experimental parameters of the nanocomposites used in the present study

Sample # particle type	Precursor core	Precursor shell	Particle collection	Method of composite formation
#1 ZrO_2/ PMMA	$Zr[OC(CH_3)_3]_4$	MMA	Thermophoresis	No composite
#2 ZrO_2/ PMMA	$Zr[OC(CH_3)_3]_4$	MMA	In EG	In situ deposition, no composite
#3 Ta_2O_5/ PMMA	$Ta(OC_2H_5)_5$	MMA	Thermophoresis	Ex situ composite formation 80 wt% reactive resin PLEXIT 55 + 20 wt% MMA 0.1 1.0 wt% of powder introduced by a dissolver stirrer into resin, using a method described in (Ritzhaupt Kleissl et al. 2005) Casting of 1 2 mm thick block; photocuring
#4 Ta_2O_5	$Ta(OC_2H_5)_5$		In EPR 162®	In situ deposition + subsequent composite formation 0.8 wt% particles in composite 100 pbw sample in EPR 162® + 25 pbw EK943® @80°C/1 h/5°/ min
#5 a d SnO_2	$SnCl_4$		In EPR 162®	In situ deposition + subsequent composite formation a. 0.1 wt%; b. 0.2 wt%; c. 3.8 wt%; 4.6 wt% particles in sample 100 pbw sample in EPR 162® + 25 pbw EK943® @80°C/1 h/5°/ min
#6 Fe_2O_3/ PMMA	$Fe(CO)_5$	MMA	Thermophoresis	Ex situ composite formation 0.1 wt% particles in composite 100 pbw sample in EPR 828® + 28 pbw EK 293®
#7 Fe_2O_3	$Fe(CO)_5$		In EPR 162®	In situ deposition + subsequent composite formation 0.1 wt% particles in composite 100 pbw sample in EPR 162® + 25 pbw EK 943® @80°C/1 h/5°/ min
#8 Fe_2O_3/ PMMA	$Fe(CO)_5$	MMA	In Cardura E10®	In situ deposition, no composite 1.57 wt% particles in sample
#9 Fe_2O_3/ PMMA	$Fe(CO)_5$	MMA	In Cardura E10® (73 wt%) + EPR 162® (27 wt%)	In situ deposition 2.1 wt% particles in sample
#10 Fe_2O_3/ ZrO_2	$Fe(CO)_5$	$Zr[OC(CH_3)_3]_4$	In Cardura E10® (73 wt%) + EPR 162® (27 wt%)	In situ deposition 0.1 wt% particles in sample
#11 Fe_2O_3/ TiO_2	$Fe(CO)_5$	$Ti[OCH(CH_3)_2]_4$	In Cardura E10® (73 wt%) + EPR 162® (27 wt%)	In situ deposition 0.3 wt% particles in sample

MMA Methylmethacrylate, *EG* Ethylene glycol, *EPR 162®* EPOKOTE resin 162, *EPR 828®* EPIKOTE Resin 828 LVEL; both epoxy resins supplied from Hexion Specialty Chemicals, *Cardura E10®* reactive diluent supplied from Hexion Specialty Chemicals, *EK 943®* EPIKURE curing agent 943 a cycloaliphatic polyamine hardener and *EK 293®* EPIKURE curing agent 293 an aminic hardener; both curing agents supplied from Hexion Specialty Chemicals, *pbw* parts by weight

2.3 Characterization methods

The particle and agglomerate characterization for the powder samples and the composites was done using TEM as well as scanning transmission electron microscopy (TEM/STEM, FEI Tecnai F20 ST). For composite characterization, 70 nm thin sections were prepared by ultramicrotomy (Leica Ultracut UCT). Powder samples and composite thin sections were prepared on copper grids coated with holey carbon film. The liquids with in-situ deposited nanoparticles were characterized using rheology measurements (Bohlin Gemini 200 HR nano) and dynamic light scattering (DLS, Cordouan DL-135). The refractive indices of the composites were determined with an Abbé refractometer (@589 nm, Krüss ar2008), transmittance was determined using a UV/Vis spectrometer for 633 nm (Hitachi U-3010) and a getSpec NIR 1.7-128-TS for NIR examination. Mechanical properties of the composites like Martens hardness (H_M) and indentation modulus (E_{IT}) were measured according to DIN EN ISO 14577 (Fischerscope

Table 2 Relevant physical data of the used components as bulk materials

Liquid	Density ρ (g/cm^3)	Refractive Index n	Viscosity η (mPa s)
Fe_2O_3[a]	4.5 5.3	2.9 3.0	
SnO_2[a]	6.8 7.1	2.0	
Ta_2O_5	8.2[a]	2.1[b]	
TiO_2[a]			
Anatase	3.8 4.0	2.5	
Rutile	4.2 5.1	2.6 2.9	
ZrO_2[a]	5.5 6.0	2.1 2.2	
MMA[c]	0.94 @25°C	1.412 @25°C	0.53 @25°C
PMMA[d]	1.19	1.49 @25°C	
Ethylene glycol (EG)[c]	1.115 @20°C	1.430 @20°C	17 @25°C
EPR 162®[e]	1.16 1.18 @20°C	1.568 ± 0.003 @25°C	4,500 ± 500 @25°C
EPR 828®[e]	1.17 ± 0.01 @ 20°C	1.572 ± 0.003 @25°C	10,000 ± 2,000 @25°C
Cardura E10®[e]	0.945 0.965 @25°C[e]	1.44 @25°C[f]	7 @23°C[e]
EK 293®[e]	0.96 ± 0.02 @ 20°C	1.4655 ± 0.002 @25°C	25 ± 10 @25°C
EK 943®[e]	0.92 ± 0.02 @ 20°C	1.487 ± 0.002 @25°C	13 ± 2 @25°C

[a] Weast et al. (1964)

[b] Szabó et al. (2008)

[c] Dow Chemical Company

[d] Weaver et al. (1995)

[e] Supplier information

[f] Measured with Abbé refractometer

HP 100 V). The determination of nanoparticle content in the liquids and composites was done by gravimetric analysis through combustion for the in-situ deposited nanoparticles, and by weighted samples in the case of ex-situ composite formation.

3 Results and discussion

3.1 Principal feasibility of in-situ deposition

The first step in the experimental series of particle synthesis and composite formation was to investigate the principal successful feasibility of the in-situ deposition of nanoparticles in a liquid. Figure 3 compares thermophoretically collected ZrO_2/PMMA nanoparticles with ZrO_2/PMMA nanoparticles directly deposited in ethylenglycole (EG). EG was used since it fulfils the requirement of a high boiling liquid combined with a relatively low viscosity (Table 2). Additionally, EG is of technological interest e.g. as a component for inks in ink jet printing.

The thermophoretically collected powder is agglomerated by van-der-Waals forces. These forces have to be overcome by the application of shear forces to reduce the size of agglomerates in suspensions. The nanoparticles deposited directly in EG have reduced agglomerate sizes because particles are collected in the liquid before they touch each other in the gas stream. Compared to typical commercial nanoparticles the microwave plasma synthesized particles are significantly smaller with narrower particle size distribution (compare to Fig. 1).

From the exemplary images it is clear, that the in-situ deposition of nanoparticles made by a physical gas phase process is a promising way for the development of optical microsystems. It is possible to produce nanoparticles with small primary particle size, narrow particle size distribution, and reduced size of agglomerates in suspension. With such materials, limitations of application potential are reduced.

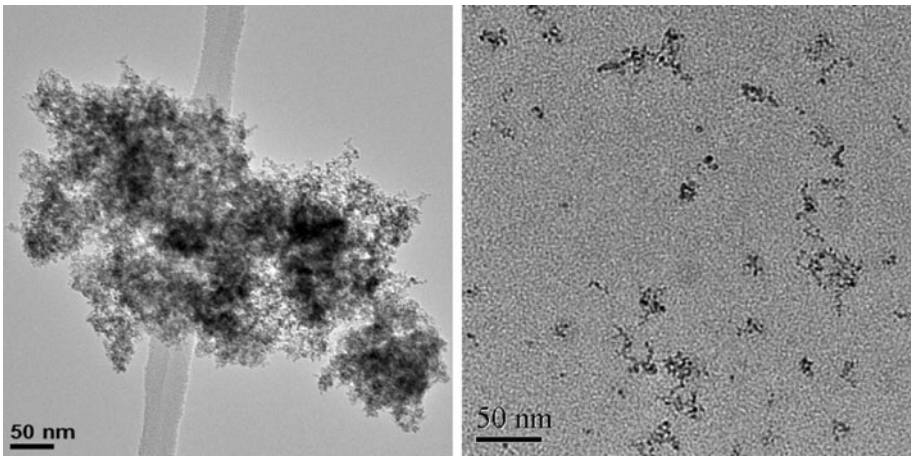

Fig. 3 TEM images of agglomerates showing thermophoretically collected ZrO_2/PMMA nanopowder (sample #1, *left*) and ZrO_2/PMMA nanopowder in situ deposited in EG (sample #2, *right*). The *left* agglomerate is only partly visible, and therefore is much larger than shown here. The primary particle size in both cases is around 4 5 nm with a narrow size distribution

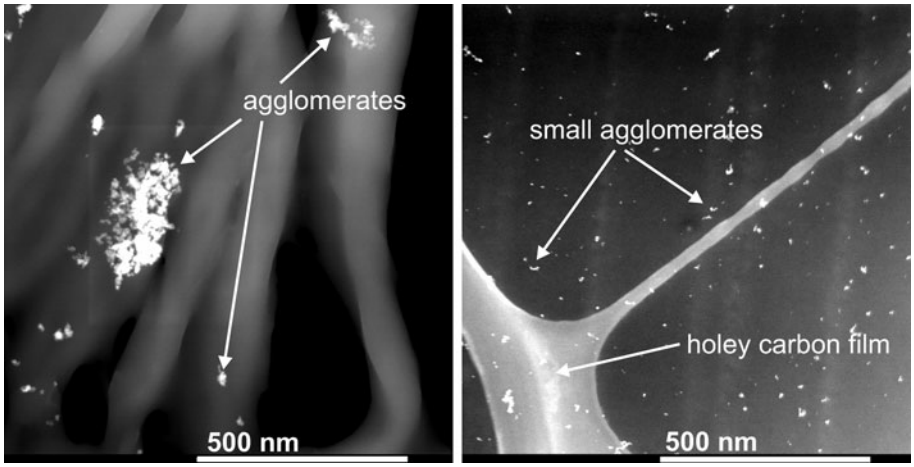

Fig. 4 STEM images of nanocomposites made using 1 wt%Ta_2O_5/PMMA nanoparticles (sample #3) with ex situ composite formation (*left*), and 0.8 wt% of in situ deposited Ta_2O_5 nanoparticles into EPR 162® (sample #4). The primary particle size of the Ta_2O_5 nanoparticles in both cases is around 4 5 nm. In the *left image* smaller agglomerates as well as larger agglomerates can be seen, whereas the *right image* shows small agglomerates, well distributed over the sample

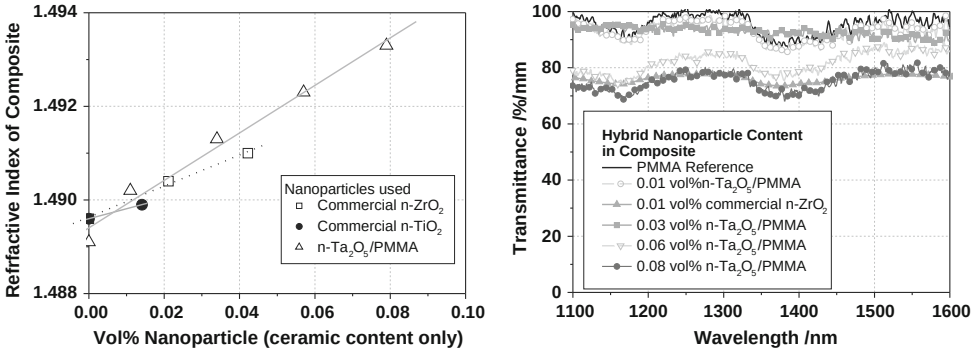

Fig. 5 Refractive index (*left*) and transmittance in the NIR (*right*) of nanoparticle/polymer nanocomposites made by ex situ methods. Data are taken from Böhm et al. (2004) and Szabó et al. (2008)

Comparing composites made by traditional ex-situ methods with composites made by the in-situ deposition method, significant differences are found concerning agglomerate size in the subsequent cured composites. This is shown exemplarily in Fig. 4. In the left image larger agglomerates as well as smaller ones can be seen. The right image shows only smaller agglomerates, finely dispersed in the polymer. From the left image it is clear, that optical properties as the transmittance might be reduced in a 2 mm thick sample (Szabó et al. 2008).

3.2 Optical properties of Ta_2O_5 and SnO_2 containing composites

In micro-optics mainly two different components are of interest: first, free space optical elements like lenses or prisms need an inherent optical refractive index as high as possible e.g. for application in instruments for microinvasive surgery. Second, the core of polymer waveguides requires only a small refractive index increase (0.005 for single mode waveguides) relative to the cladding material for successful light-guiding. Polymer waveguides can be used as optical passive devices like beam splitters or as polymer optical fibers, in both cases they show several advantages like reduced weight and easier processing in comparison to the established glass-based systems.

The modification of the refractive index with coeval preservation of the transmittance is therefore one of the challenges for particle/matrix nanocomposites. Measurements of optical properties of the Ta_2O_5/PMMA nanocomposites (sample #3) show very promising results for application in micro optics. The refractive indices, determined at 633 and 1550 nm, respectively, are increasing with increasing hybrid-powder content. This is shown, in comparison to commercial nanopowders, in Fig. 5 (left). As the difference of refractive indices between the polymer and the Ta_2O_5 is quite high, the increase of the refractive index for the composites is visible even at low nanoparticle contents. The achieved increase of refractive index is slightly higher than the increase observed in composites with commercial ZrO_2 (primary $d_{50} = 30$ nm, $n = 2.2$) at comparable weight contents (Böhm et al. 2004). The increase of refractive index is significantly higher than that observed with commercial Al_2O_3-C (primary $d_{50} = 13$ nm, $n = 1.76$, Evonik Degussa GmbH) at higher weight fraction (Böhm et al. 2004). This is evident, because the refractive index of Al_2O_3-C is lower than the refractive index of Ta_2O_5. The missing values for higher particle

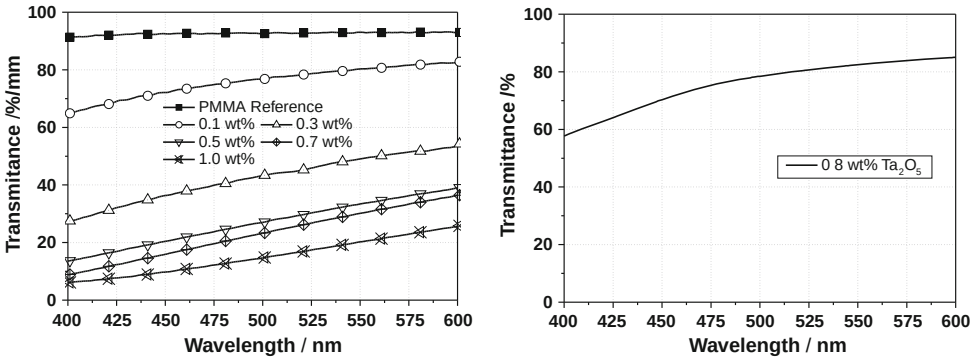

Fig. 6 Comparison of transmittance in the Vis range. Conventionally ex situ produced nanocomposite (*left*, sample #3), in situ deposited nanoparticles in EPR 162 (*right*, sample #4)

concentrations in case of commercial nanoparticles (Fig. 5) are caused by a breakdown in transmission.

For the ex-situ Ta_2O_5-composite the transmittance is only slightly depressed compared to the pure resin up to a nanoparticle concentration of 0.03 vol% (Fig. 5, right). Hence, for small hybrid nanoparticle content the process of ex-situ particle incorporation works well. With increasing hybrid nanoparticle content up to 0.1 vol% the transmittance is reduced. However, compared to nanocomposites made of PMMA and commercial ZrO_2 nanoparticles (Böhm et al. 2004) the transmittance of the Ta_2O_5-nanocomposite is less reduced at comparable particle concentrations. Transmittance measurements in the Vis-range show significant differences when comparing ex-situ composite formation method (sample #3) and in-situ deposition of nanoparticles (sample #4). This is shown in Fig. 6. The transmittance in the Vis-range is strongly degraded, even at very low particle load in the ex-situ fabricated composite. In case of the in-situ deposited nanoparticles the transmittance in the Vis-range is significantly improved due to the smaller aggregate size (see Fig. 4, right). The observed changes regarding refractive indices (Fig. 5) are very well suited for polymer waveguides. Additionally, for applications in microoptics the resulting optical transmittance in the visible, e.g. for consumer electronics, and NIR-range, for optical data transmittance using the standard telecommunication wavelength at 1,310 and 1,550 nm, is also of particular interest.

In literature particle loads in the range of 10 to 50 wt% are standard, e.g. for TiO_2, leading to substantial changes of the refractive index (Nussbaumer et al. 2003; Guan et al. 2006; Nakayama and Hayashi 2007; Zhang et al. 2007). But, the authors only measure the transmittance using thin films. At larger sample thickness the transmittance drops significantly due to primary particle agglomeration and prevents the use of the composites in optical devices. Therefore, the published data have to be carefully controlled with respect to the measured sample thickness. A thin layer of a few 100 nm thickness can exhibit excellent optical transmittance values in the visible, which drops almost to zero considering technical dimensions of some mm used in the ASTM standard for transmittance measurements applying Lambert Beers-law.

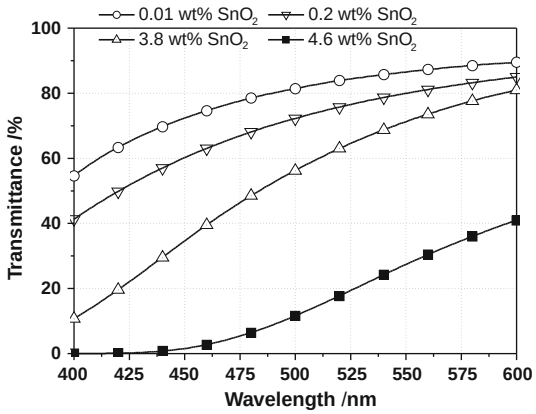

Fig. 7 Transmittance in the Vis range for SnO_2 nanoparticles in situ deposited into EPR 162® (sample #5 a d)

Using the in-situ deposition of particles into liquids the attainable particle concentration is not limited below 1 wt%. In case of SnO_2 nanoparticles (Fig. 7, sample #5 a d) a reasonable transmittance in the Vis-range is measured until a particle load of 3.8 wt%. The fading at higher particle loads may be due to starting slight optical degradation of the EPR-162®.

3.3 Fe_2O_3-containing nanocomposites for electromagnetic wave absorbtion

Regarding application of nanoparticles as additives for improved microwave curing of resins the distribution of dielectric active nanoparticles is crucial to avoid the formation of hot-spots during the microwave heating (Schlabach et al. 2009). For this application it is also necessary to achieve a homogeneous distribution of nanoparticles in the composite. The enhancement of nanoparticle distribution is exemplarily shown in Fig. 8 for Fe_2O_3/PMMA nanoparticles dispersed ex-situ in

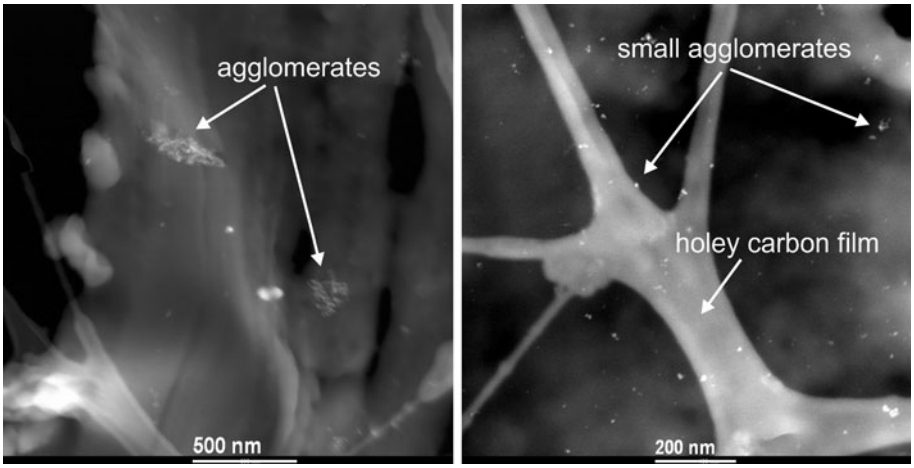

Fig. 8 STEM images of nanocomposites using Fe_2O_3/PMMA hybrid nanoparticles (sample #6), or Fe_2O_3 nanoparticles (sample #7). The *left image* shows an ex situ produced nanocomposite with 0.1 wt% hybrid nanoparticles, containing larger agglomerates. The *right image* shows a composite produced by in situ deposition of hybrid nanoparticles in EPR 162® with subsequent composite formation. The resulting composite contains approximately 0.1 wt% nanoparticles

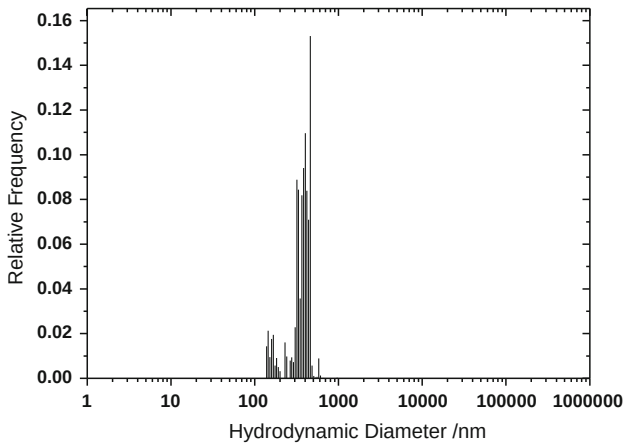

Fig. 9 Particle size distribution measured by dynamic light scattering of nanoparticles in situ deposited in reactive diluent Cardura E10® (sample #8). For DLS measurement the sample was diluted with Cardura E10® to reduce particle interaction effects. The given values are Mie corrected

EPR-828® and Fe_2O_3/PMMA nanoparticles dispersed in-situ in EPR-162® with subsequent composite formation, respectively.

As EPR-162® is a highly viscous liquid (4,500 mPa s @25°C) in-situ particle deposition is not optimal. One possibility to circumvent the problem of high viscosity during nanoparticle precipitation is to use a reactive diluent with low viscosity such as Cardura E10® (7 mPa s @23°C). This reactive diluent will be part of the composite, as it reacts with the resin. The resulting particle size distribution measured with dynamic light scattering is shown for sample #8 in Fig. 9. Depicted is the Mie-corrected hydrodynamic diameter.

3.4 Surface modification

Additional improvement of the particle/agglomerate size in liquids for the in-situ deposited particles is possible with surface modification of the nanoparticles. As an example particle size distribution for Fe_2O_3 with different coatings is shown in Fig. 10. The coating was realized using the process shown in Fig. 2. In case of PMMA-coating MMA as precursor was directly introduced after the reaction zone and condenses on the previously formed nanoparticles followed by polymerization due to UV-light from the plasma. In case of ZrO_2- and TiO_2-coating, appropriate precursors were introduced after the reaction zone followed by a second plasma using a consecutive reaction zone (Vollath and Szabó 2006). All samples were in-situ deposited into a mixture of the resin EPR-162® (27 wt%) and the reactive diluent Cardura E10® (73 wt%). For F_2O_3/PMMA a very narrow agglomerate size distribution is visible with a d_{50} value of the hydrodynamic diameter of around 115 nm (Fig. 10). The agglomerate size distribution is more obvious in the cumulative curve showing a steep increase (Fig. 10, right). For the ZrO_2- and TiO_2-coated nanoparticles the size distribution is broader but the d_{50} values are smaller with around 100 nm for the ZrO_2-coated particles and around 40 nm for the bimodal distributed particles with TiO_2-coating.

3.5 Influence of nanoparticles on rheological and mechanical properties

Besides the size of nanoparticles and their distribution in composites, both directly related to physical properties like optical, or microwave absorbing properties, also rheological

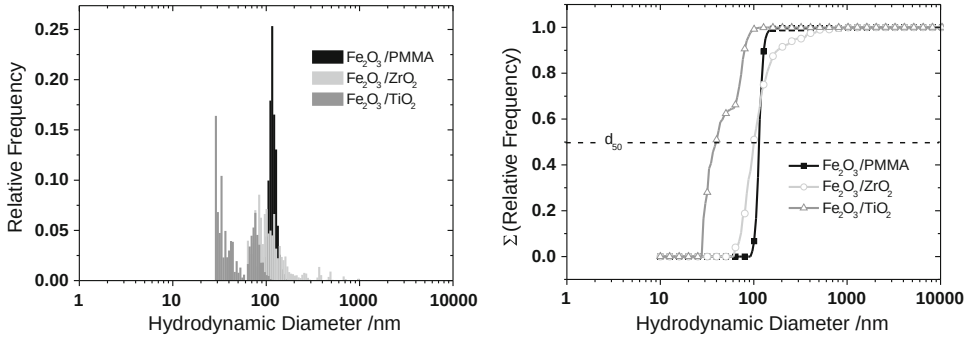

Fig. 10 Particle size distribution of different surface modified Fe_2O_3 nanoparticles (samples #9 11) directly deposited into a mixture of Cardura E10® (73 wt%) and EPR 162® (27 wt%). The hydrodynamic diameter is shown as a histogram (*left*) as well as a cumulative curve (*right*). The *horizontal line* in the *right image* represents the d_{50} value. For measurement the samples were diluted with Cardura E10® to reduce particle interactions. The given values are Mie corrected

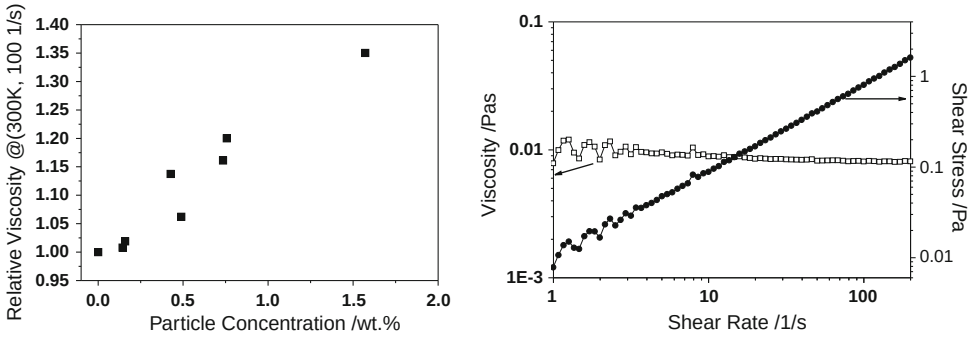

Fig. 11 Relative viscosity with increasing particle load (*left*) and viscosity as well as shear stress versus shear rate indicating a Newtonian flow behaviour (*right*) exemplarily shown for sample #8

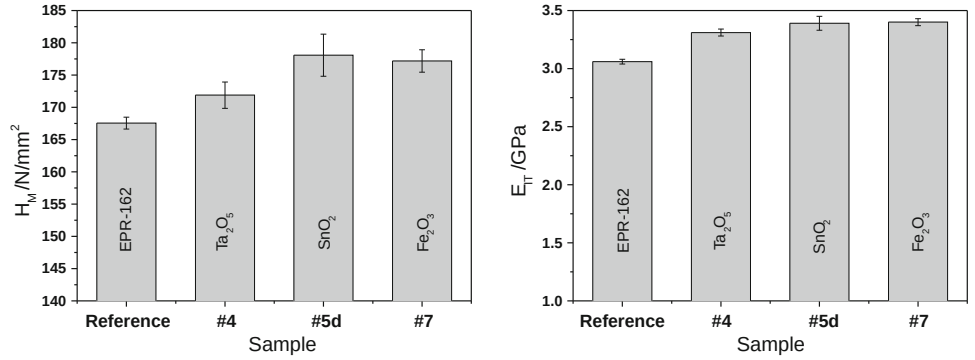

Fig. 12 Martens hardness H_M (*left*) and indentation modulus E_{IT} (*right*) of different nanoparticle filled nanocomposites. As a reference, hardness of the pristine epoxy resin EPR 162® is also given. An enhancement of hardness and indentation modulus by using different filler is visible

and mechanical properties of the composite will play an important role regarding the processability as well as applicability of a material. The influence of particle load on rheology is exemplarily given for sample #8 in Fig. 11. The relative viscosity, defined as viscosity of the mixture/viscosity of the pure compound, increases with increasing particle load, as the interface area in the composite increases significantly with increasing particle load. The increase of viscosity at the given particle concentration is in good agreement with data obtained from composites using commercial Al_2O_3-nanoparticles (Hanemann 2008). The flow behaviour is a classical Newtonian, since the viscosity is independent of the shear rate and the shear stress is a linear (Fig. 11, right).

The possible effect on mechanical composite properties is shown in Fig. 12. Compared to the pure cured resin several nanoparticle modified cured resins show an influence regarding H_M (Fig. 12, left) as well as on the E_{IT} (Fig. 12, right). Even with a relatively small particle load (see Table 1) the influence on mechanical properties is visible.

However, a direct correlation between particle load and mechanical properties is not observable. The kind of material seems to be important, too. The final assessment

of such values will depend on the different possible application areas.

4 Summary and conclusions

We demonstrated the benefit of combining the microwave plasma process for nanoparticle synthesis with an in-situ deposition method in liquids regarding the resulting agglomerate size in polymer-matrix composites. As the microwave plasma process yields in primary particle sizes below 10 nm with narrow particle size distribution, and as the particles are collected in the liquid before they can touch each other in the gas stream, tendency for the formation of agglomerates is drastically reduced. TEM as well as dynamic light scattering measurements are in good agreement regarding the size of agglomerates. The observed changes of refractive indices are very well suited for polymer waveguides and the resulting optical transmittance in the visible an NIR-range is interesting for applications for consumer electronics or optical data transmittance. The prepared liquids show Newtonian flow behaviour while the viscosity increases with increasing particle load, even at low particle concentrations. An influence of nanoparticles on mechanical properties was also observed.

The achieved particle distribution in the composites opens potential applications in microoptics, microwave curing, or ink-jet printing. Further improvement with respect to increasing nanoparticle content and optimized composite formation is necessary. Additionally, one has to think about combining surface functionalization of the nanoparticles using surfactants with in-situ deposition in liquids to further reduce the agglomerate size.

Acknowledgments The authors thank Ivonne Fuchs, Katharina Giemza and Friedrich Wacker for technical support. Finally the authors appreciate support of Hexion Specialty Chemicals with resins, hardener and reactive diluent.

References

Althues H, Henle J, Kaskel S (2007) Functional inorganic nanofillers for transparent polymers. Chem Soc Rev 36(9):1454 1465

Böhm J, Haußelt J, Henzi P, Litfin K, Hanemann T (2004) Tuning the refractive index of polymers for polymer waveguides using nanoscaled ceramics or organic dyes. Adv Eng Mater 6(1 2):52 57

Caseri WR (2006) Nanocomposites of polymers and inorganic particles: Preparation, structure and properties. Mater Sci Technol 22(7):807 817

Doak J, Gupta RK, Manivannan K, Ghosh K, Kahol PK (2010) Effect of particle size distributions on absorbance spectra of gold nanoparticles. Physica E 42(5):1605 1609

Feher LE (2009) Energy efficient microwave systems materials processing technologies for avionic, mobility and environmental applications. Springer, Berlin

Guan C, Lu CL, Liu YF, Yang B (2006) Preparation and character ization of high refractive index thin films of TiO_2/epoxy resin nanocomposites. J Appl Polym Sci 102(2):1631 1636

Han DH, Wang JP, Luo HL (1994) Crystallite size effect on saturation magnetization of fine ferrimagnetic particles. J Magn Magn Mater 136(1 2):176 182

Hanemann T (2008) Influence of particle properties on the viscosity of polymer alumina composites. Ceram Int 34:2099 2105

Hanemann T, Szabó DV (2010) Polymer nanoparticle composites: from synthesis to modern applications. Materials 3(6):3468 3517

Hanemann T, Haußelt J, Ritzhaupt Kleissl E (2009) Compounding, micro injection moulding and characterisation of polycarbonate nanosized alumina composites for application in microoptics. Microsyst Technol 15(3):421 427

Kruis FE, Fissan H, Peled A (1998) Synthesis of nanoparticles in the gas phase for electronic, optical and magnetic applications a review. J Aerosol Sci 29(5 6):511 535

Kyprianidou Leodidou T, Caseri W, Suter UW (1994) Size variation of PbS particles in high refractive index nanocomposites. J Phys Chem 98(36):8992 8997

Lamparth I, Szabó DV, Vollath D (2002) Ceramic nanoparticles coated with polymers based on acrylic derivatives. Macromol Symp 181:107 112

Li W, Ni C, Lin H, Huang CP, Shah SI (2004) Size dependence of thermal stability of TiO_2 nanoparticles. J Appl Phys 96(11): 6663 6668

Luca V (2009) Comparison of size dependent structural and elec tronic properties of anatase and rutile nanoparticles. J Phys Chem C 113(16):6367 6380

Nakayama N, Hayashi T (2007) Preparation and characterization of TiO_2 and polymer nanocomposite films with high refractive index. J Appl Polym Sci 105(6):3662 3672

Nienhaus H, Kravets V, Koutouzov S, Meier C, Lorke A, Wiggers H, Kennedy MK, Kruis FE (2006) Quantum size effect of valence band plasmon energies in Si and sno_x nanoparticles. J Vac Sci Technol B 24(3):1156 1161

Nussbaumer RJ, Caseri WR, Smith P, Tervoort T (2003) Polymer TiO_2 nanocomposites: A route towards visually transparent broadband UV filters and high refractive index materials. Macromol Mater Eng 288(1):44 49

Paul DR, Robeson LM (2008) Polymer nanotechnology: nanocom posites. Polymer 49(15):3187 3204

Qi WH, Wang MP (2005) Size and shape dependent lattice parameters of metallic nanoparticles. J Nanopart Res 7(1):51 57

Ritzhaupt Kleissl E, Böhm J, Hausselt J, Hanemann T (2005) Process chain for tailoring the refractive index of thermoplastic optical materials using ceramic nanoparticles. Adv Eng Mater 7(6):540 545

Schlabach S, Szabó DV, Feher L (2009) Microwave plasma synthesized nanoparticles. In: Feher L (ed) 12th international conference on microwave and high frequency heating (AMPERE 2009), Karlsruhe. Karlsruhe Institute of Technology (KIT), pp 144 147 (CD ROM)

Szabó DV, Ochs R, Schlabach S, Ritzhaupt Kleissl E, Hanemann T (2008) New core/shell Ta_2O_5 PMMA nanocomposites for applications as polymer waveguides, Materials Research Society Symposium Proceedings, vol 1056E. In: Nanophase and nano composite materials V. Materials Research Society, Warrendale, PA, paper 1056 HH10 9

Vollath D, Szabó DV (1999) Coated nanoparticles: a new way to improved nanocomposites. J Nanopart Res 1:235 242

Vollath D, Szabó DV (2006) The microwave plasma process a versatile process to synthesise nanoparticulate materials. J Nano part Res 8(3 4):417 428

Vollath D, Szabó DV, Fuchs J (1999) Synthesis and properties of ceramic polymer composites. Nanostruct Mater 12(1 4): 433 438

Weast RC, Selby SM, Hodgman CD (1964) Handbook of chemistry and physics, 45th edn. The Chemical Rubber CO, Cleveland

Weaver KD, Stoffer JO, Day DE (1995) Interfacial bonding and optical transmission for transparent fiberglass/poly(methyl meth acrylate) composites. Polym Composite 16(2):161 169

Zhang M, Lin GQ, Dong C, Wen LS (2007) Amorphous TiO_2 films with high refractive index deposited by pulsed bias arc ion plating. Surf Coat Tech 201(16 17):7252 7258

Zhang HZ, Chen B, Banfield JF (2009) The size dependence of the surface free energy of titania nanocrystals. Phys Chem Chem Phys 11(14):2553 2558